• Article •

Advances in Polar Science

doi: 10.3724/SP.J.1085.2011.00010

March 2011 Vol.22 No.1: 10–16

Investigation of the thermodynamic processes of a floe-lead system in the central Arctic during later summer

LEI RuiBo[1*], LI ZhiJun [2], CHENG Bin[3], YANG QingHua[4] & LI Na [1]

[1] Polar Research Institute of China, Shanghai 200136, China;
[2] State Key Laboratory of Coastal and Offshore Engineering, Dalian University of Technology, Dalian 116024, China;
[3] Finnish Meteorology Institute, P.O.Box33, Helsinki, FI−00931, Finland;
[4] National Marine Environmental Forecasting Center, Beijing 100081, China

Received November 19, 2010; accepted January 26, 2011

Abstract Thermodynamic processes of a system involving a floe and a small lead in the central Arctic were investigated during the ice-camp period of the third Chinese National Arctic Research Expedition from 20 to 28 August, 2008. The measurements included surface air temperatures above the floe, spectral albedo of the lead, seawater temperatures in the lead and under the ice cover, and the lateral and bottom mass balance of the floe. The surface air temperature at 1.15 m remained below 0℃throughout the observation period and sea ice had commenced its annual cycle of growth in response to autumn cooling during the study. The surface of the lead was frozen by 23 August, after which the spectral albedo of the thin-ice-covered lead in the band of 320−950 nm was 0.46 ±0.03, the seawater temperatures both in the lead and under the ice cover, as well as the vertical seawater-temperature gradient in the lead decreased gradually, and the oceanic heat under the ice was maintained at a low level approaching 0 W/m^2. By the end of the measurement, the thickness of the investigated floe had reached its annual minimum, while the lateral of the floe was still in the melting phase, with a mean melting rate of 1.0 ±0.3 cm/d during the measurement, responding to an equivalent latent heat flux of 21 ±6 W/m^2. The lateral melting of the floe had made a more significant contribution to the sea-ice mass balance than the surface and bottom melting in the end of August.

Keywords **Sea ice, lead, thermodynamic process, temperature, thickness, Arctic**

Citation: Lei R B, Li Z J, Cheng B, et al. Investigation of the thermodynamic processes of a floe-lead system in the central Arctic during later summer. Adv Polar Sci, 2011, 22：10—16, doi: 10.3724/SP.J.1085.2011.00010

0 Introduction

Sea ice is a key component in climate system and has long been recognized as a significant indicator of local and global climate change. Both the extent and the thickness of sea ice in the Arctic Ocean had decreased in the last decade [1−2]. Specifically the extent and area of Arctic sea ice reached their minimal values since the beginning of satellite-remote-sensing era on 14 September 2007[1]. An increasing number of characteristics of Arctic sea ice have been found to be influenced by climate change, such as more significant melt-pond coverage and greater lead fraction during summer [3]. These changes result in the introduction of more solar irradiance absorbed by the ocean, which in turn accelerate the sea-ice melting [4]. These changes also lead to the introduction of a sea-ice surface with a spatial multiplex condition to reach to higher latitude, complicate the parameterization of surface heat flux for climate models and increase the challenge for forecasting sea-ice evolvement in the Arctic Ocean [5].

The thermodynamic interaction between floe and lead is crucial for the coupling process involving the atmosphere, sea ice and ocean. Its parameterization has been included in mathematic models since as early as the 1970s[6]. To date, multiform techniques have been devolved to measure the sea-ice mass balance and energy fluxes at the interfaces

* Corresponding author (email: leiruibo@pric.gov.cn)

between the atmosphere and snow/ice, as well as between ice and the ocean [7–10]. When compared to those mea- surements, similar measurements of the thermo-dynamic interaction between floe and lead are deficient. The spatial variations in the seawater temperature under ice cover from a lead to the centre of a floe was investigated by Li et al. during the camp period of the second Chinese National Arctic Research Expedition (CHINARE-Arctic)[11]. However, no measurement of the lateral mass balance of a floe adjacent to a lead has been conducted to date.

Based on the technique introduced by Li et al. [11], a more sophisticated system that includes measurement of the surface air temperature above a floe, spectral albedo of a lead, seawater temperatures in a lead and under a floe, and the lateral and bottom mass balance of a floe was developed and utilized to investigate the thermodynamic interaction between a floe and a small lead during the camp period of the third CHINARE-Arctic cruise in the summer of 2008. The scheme of the measurement system, the measurement process and the primary results are introduced in the current study.

1 Field work

1.1 Ice camp and weather conditions

Figure 1 shows the cruise trajectory (blue line indicates the northward navigation, green line indicates the southward navigation) of the R.V. Xuelong in the sea-ice zone during the third CHINARE-Arctic cruise. Also shown is the drift track of the ice camp and sea-ice concentration on 25 August. The ice concentration was derived from Advanced Microwave Scanning Radiometer-EOS (AMSR-E). The investigated regions for the sea-ice physical study included the Chukchi Sea, Beaufort Sea and the central Arctic. The Xuelong sailed into the sea-ice zone on 4 August 2008, and reached 84.6 ºN, 144.7 ºW on 19 August, at which time the ice camp was set up on a relatively large multiyear floe with a diameter of about 1.5 km. Subsequently, the ice camp was transported to 85.2 °N, 147.3 °W by the Transpolar Drift northwestward until 28 August, 2008, when the ice camp was retracted. Thus, the local time at 146 °W is defined for all measurements in the current study.

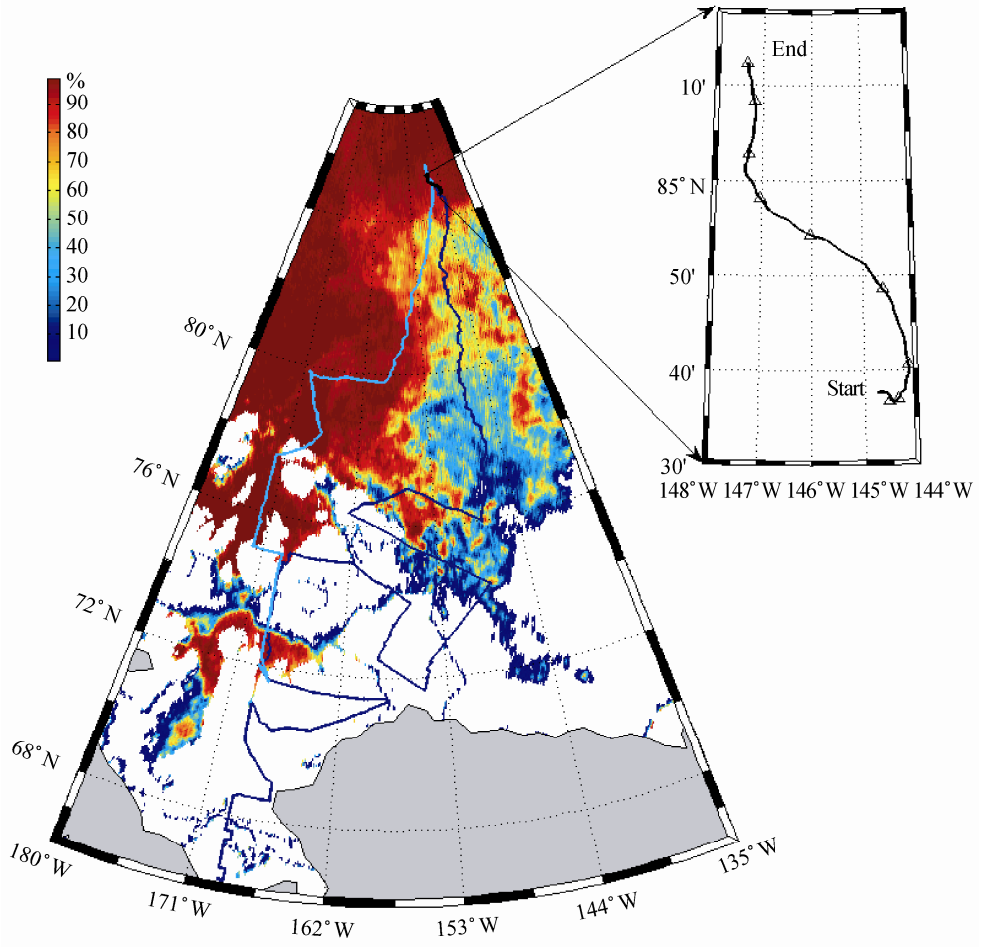

Figure 1 The cruise trajectory of the Xuelong and the drift trajectory of the ice camp (daily location is marked by triangle).

There was a large spatial variation in the ice thickness of the camp floe, with a mean value of 4.19 ±1.33 m. The average snow depth was 0.07±0.02 m, with a new-snow surface layer of about 3—5cm. Ice-core measurements showed that the vertical average ice temperature was −1.71℃, and its vertical temperature gradient approached 0 K/m, which is similar to the temperature-profile pattern of summer landfast ice in Antarctica[12]. The ice core showed low salinity and density, with vertical average values of 0.8 PSU and 621 kg/m^3, respectively. Most brine channels were connected as the destroying of ice crystal, thus, the porosity of ice was larger during the cruise than during winter. Helicopter observations on 19 August in the region around the ice camp with a diameter of 10 km showed that there were no floes with a size larger than 2 km^2, and that the lead fraction and melt pond coverage were quite large, with ice concentration of 87% and melt pond coverage of 27%. Overcast sky was prevalent for the entire camp period, with some slight snowfall and sleet events occurring.

The surface air temperature at an altitude of 1.15 m remained below 0℃during the camp period, with a mean and minimum of −1.59℃ and −3.97℃, respectively. The wind speed increased gradually from 22 August onward, and reached to its maximum of 7.8 m/s at 14:44 on 24 August. The wind made a large contribution to the spatial redistribution of snow cover.

1.2 Design scheme of the measurement system and the measurement process

As shown in Figure 2, the deployment position was related to a small lead with a width ranging from 1.00 to 2.00 m, and the width of the deployment position was 1.20 m. A pair of TriOS (Oldenburg, Germany) RAMSES ACC-2 VIS hyper-spectral radiometers (hereafter referred to as RAMSES) was used to measure the incident irradiance and the upwelling reflected irradiance. The RAMSES sensor is equipped with a cosine collector to detect irradiance ranging from 320 to 950 nm, and the field of view is a full hemisphere. This sensor has an average spectral resolution of 3.3 nm, with a sensitivity as low as 4×10^{-5} W/(m^2 · nm) and a spectral accuracy of 0.3 nm. Detailed technical specifications can be found in Nicolaus et al.[13]. The RAMESE sensors were fixed on a horizontal bar at 0.80 m above the lead.

PT100 sensors (JUMO, Dalian, China) were used to measure the air temperature and seawater temperature. The sensors were calibrated to an accuracy of ±0.1 K prior to deployment. The coherence of these sensors was controlled by selecting sensors that had readings within ±0.05 K of each other during calibration. The sensor (marked by **C** in Figure 2) used to measure the surface air temperature was set up at 1.15 m above the ice surface. The thermistor string deployed in the lead (marked by **T1** in Figure 2) was composed of 15 sensors at depths of 0.20, 0.40, 0.70, 1.00, 1.50, 2.00, 2.50, 3.15, 4.15, 5.15, 6.15, 7.15, 9.15, 11.15 and 13.15 m, respectively. There are two thermistor strings deployed under the ice cover (marked **T2** and **T3** in Figure 2),which both contained eight sensors at depths of 3.15, 4.15, 5.15, 6.15, 7.15, 9.15 , 11.15 and 13.15 m, respectively. The installation used to measure the sea-ice-lateral mass balance was composed of two

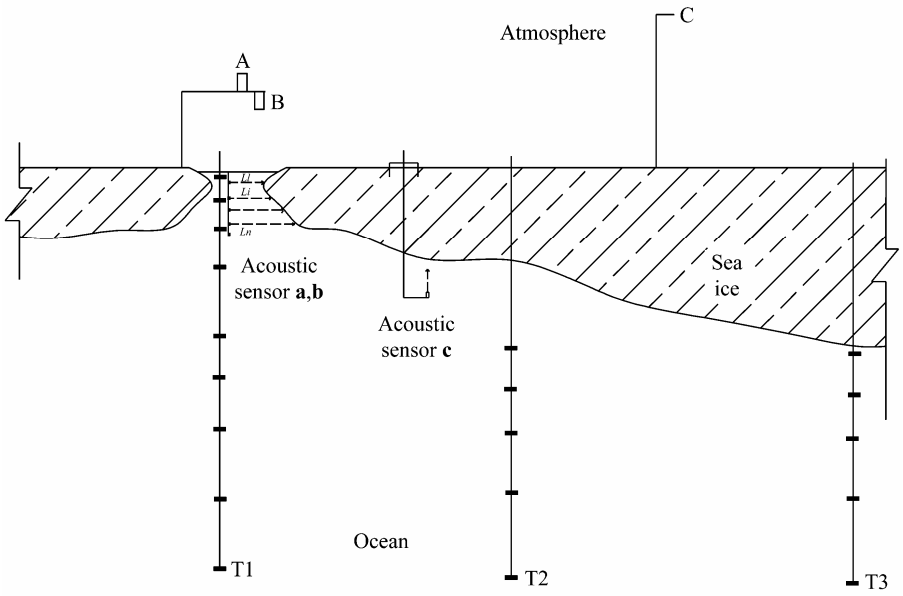

Figure 2 Observation system for the thermodynamic processes of a floe-lead system.

acoustic sensors (marked **a** and **b** in Figure 2). One sensor (**a**) was used to detect the horizontal distance between the sensor and the floe lateral profile; while the other one (**b**) was used to calibrate the data. There was a fixed baffler in front of the calibrated sensor (**b**) with a horizontal distance of 0.21 m. The acoustic speed could be derived by recording the two-way travel time between the calibrated sensor (**b**) and the baffler. The records of the measuring sensors could then be calibrated. There was an additional acoustic sensor (**c**) used to monitor the ice-bottom mass balance, which was initially deployed 0.50 m under the ice bottom and positioned to look up vertically using a folded frame. The horizontal distances from the acoustic sensor **c** and thermistor strings **T2** and **T3** to the lead edge were 7, 10 and 45 m, respectively.

The measurements of the sea-ice bottom and lateral mass balance were controlled artificially, thus, only one record per day was obtained for all sensors. All other measurements were controlled automatically with a recording interval of 10 min. All measurements lasted from 22 to 28 August, except for the spectral albedo measurements, which lasted from 25 to 28 August. Some measurements were disturbed by the polar bears during the camp period, which resulted in the loss of some data.

2 Results

2.1 Spectral albedo over the lead

The surface of the investigated lead was frozen by 23 August due to the persistent decreasing of air temperature. The new ice grew to 5.0 cm by 29 August. A thin snow cover appeared over this new ice cover due to some snowfall events, with a maximum depth of 1.0cm occurring after a snowfall event on 27 August. The time series of the spectral albedo of this thin ice cover from 23:00, 25 August to 15:30, 28 August is shown in Figure 3.

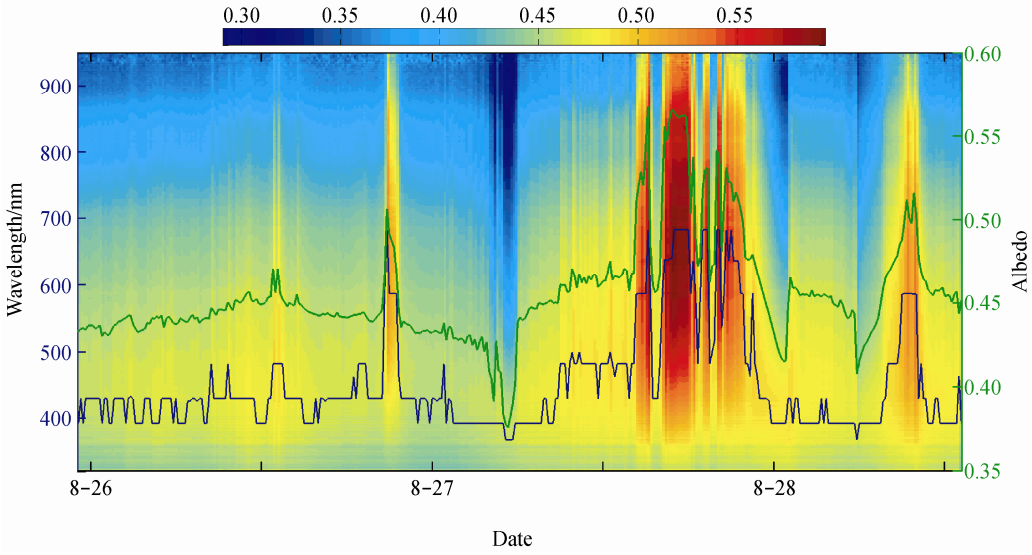

Figure 3 Spectral (color plot) and broadband (green line) albedo of the thin ice-covered lead, and the wavelength with the maximum albedo (blue line).

The broadband integrated albedo over 320 nm—950 nm ranged from 0.38 to 0.57, with a mean value of 0.46 ±0.03, which was close to the value of the refrozen melt pond [14]. This change can be related to the local synoptic process. The snowfall events that occurred on the nightfall of 26 August, the nightfall of 27 August and the morning of 28 August introduced a slight increase in the spectral albedo over the entire measurement wavelength with peaks of the broadband integrated albedo larger than 0.5. In contrast, a sleet event occurred from the night of 27 August to the early morning of 28 August, which introduced an identifiable decrease in the spectral albedo, with a valley value smaller than 0.4. The maximal spectral albedo occurred in the range of 390 nm—460 nm (blue spectrum) when there was no snow cover over the ice or only some slush over surface. It could be explained that an intense absorption of the irradiation with large wavelength by the moisture over surface would occur in these cases. In contrast, the maximum spectral albedo occurred for red spectrum when there was relatively thick dry snow over the ice.

2.2 Seawater temperature

As shown in Figure 4(b), at the beginning of the measurement, the vertical gradient of seawater temperature in the investigated lead was relatively high; with the temperature of the surface water layer at a depth of 0.2 m being distinctly warmer than that of the subsurface layer and fluctuating with the changes in the surface air

temperature. The vertical gradient of the seawater temperature in the lead decreased after freezing of the lead as shown in Figure 4(c). Although the surface air temperature increased distinctly during the nightfall of 27 August, the seawater temperature at surface layer cooled due to the increase in the surface albedo and the decrease in the irradiation transmittance in the same temporal interval. As shown in Figure 4(e), due to the influence of the lead and the upwelling of oceanic heat, there was a local minimum for temperature profile **T1** at the depth of about 4.2 m, which was also close to the average floe bottom. There was no identifiable influence of surface air temperature on the seawater temperature profile of **T2** and **T3**, as shown in Figure 4(f) and (g); and the vertical temperature gradients of **T2** and **T3** were very small, with a maximum of 0.016 K/m. These results implied that a small upwelling of oceanic heat flux occurred under the ice. These findings agree with the results estimated from the data obtained from the ice mass balance buoy[10], which had a value in the central Arctic of 3 W/m^2 by the end of August. Based on a comparison of the seawater temperatures of **T1**-**T3** at the same depth, there was no identifiable horizontal gradient. These findings differed from those of Li et al. [11], who found that there was a slight, but identifiable horizontal gradient for the seawater temperature under the ice from the floe margin close to a lead to the center of this floe. This discrepancy can be explained by their investigation having a lead with a larger size than ours, which likely had a greater influence on the thermodynamic system of seawater under the ice. Moreover, most leads around our investigated floe were frozen during our measurements, which would reduce the contribution of the leads to the vertical heat and irradiance flux transmittance in the scale of meters to kilometers.

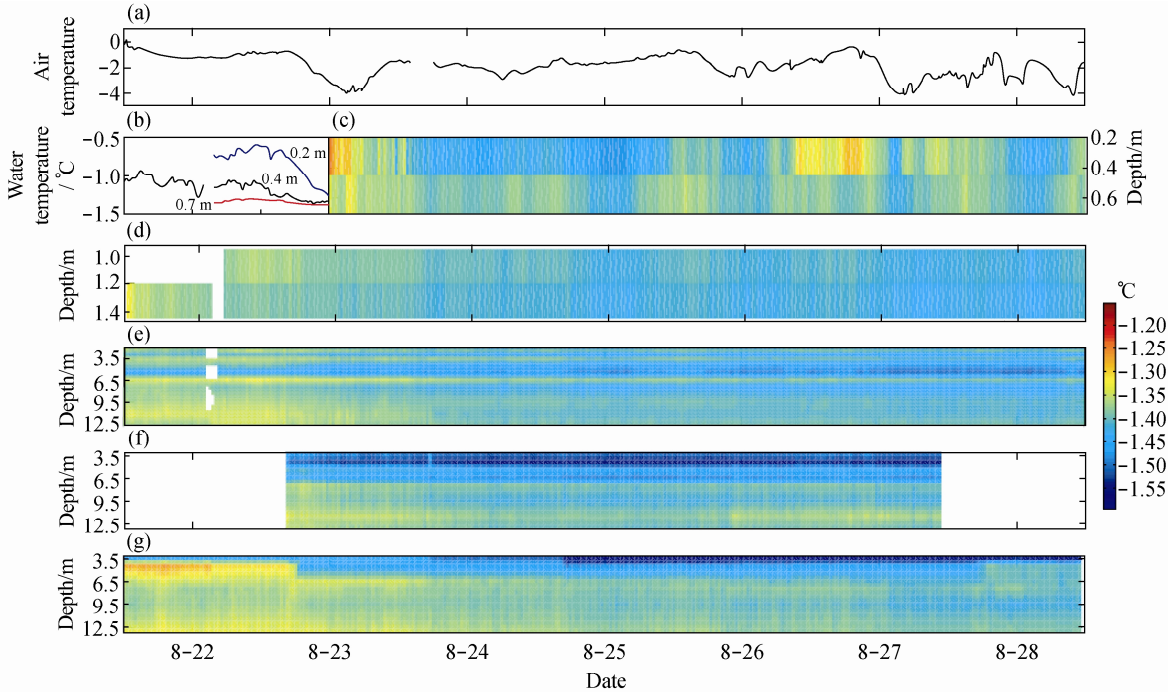

Figure 4 Surface air temperature over the floe (a), the seawater temperatures at T1 (b-e), T2 (f) and T3 (g).

2.3 Mass balance at the bottom and lateral portion of a floe

Figure 5 shows the variations in the lateral portion of the investigated floe. Valid measurements were limited to depths ranging from 16 to 66 cm, because the sensor has to be submerged under about 15 cm of seawater to receive the acoustic echo, and the inclination of the floe lateral at the bottom was beyond the valid range to reflect the incident signal to the receiving field of the acoustic sensor. There was a slight local salient at the surface layer above 21 cm. Except this part the ice lateral was characterized by a C shaped profile, with an obvious salient at a depth of 36—66 cm. These findings implied that an obvious melting occurred at the subsurface layer and ice bottom. For the subsurface layer, this likely occurred due to a local collection of the conductive heat flux at the subsurface layer during the summer melting season [12, 15]; while for the bottom layer, the melting was likely due to the combined influence of the strengthened heat conduction through the lead and the upwelling oceanic heat flux. The mean lateral melting rate of the investigated floe was 1.0 ±0.3 cm/d, which implied an equivalent latent heat flux of 21 ±6 W/m^2, as estimated by the following equation:

$$F_L = -\rho_{si} L_f \frac{\partial z_{si}}{\partial t}, \quad (1)$$

where L_f is the sea-ice latent heat of fusion, which is a function of sea-ice temperature and density[16], $(\partial z_{si}/\partial t)$ is the ice melting rate, and ρ_{si} is the bulk sea-ice density. Based on ice-core measurements, the ρ_{si} for this study can be assigned a value of 621 kg/m^3 and the L_f can be assigned a value of 3.11×105 J/kg[1]. The estimated equivalent latent heat flux was close to that responding to the Arctic sea-ice bottom melting during the advanced melting season[10].

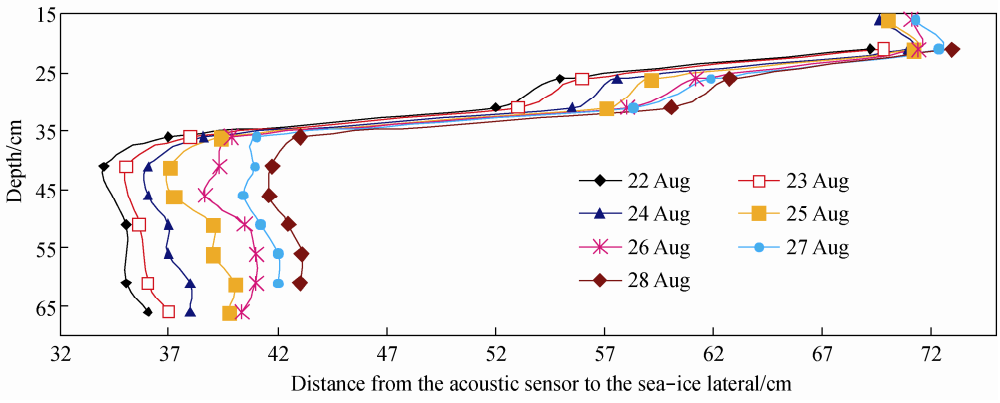

Figure 5 Variations in the floe lateral.

Figure 6 shows the variations in the base of the investigated floe. There was a melting of 1.1 cm for the floe bottom from 22 August to 26 August, when it reached its mass balance. Based on the ice-core measurement, the vertical gradient of the ice temperature was close to zero, which implied a small vertical conductive heat flux through the floe. These findings indicated that the upwelling oceanic heat flux at the ice bottom was also kept at a low level from 26 August onward.

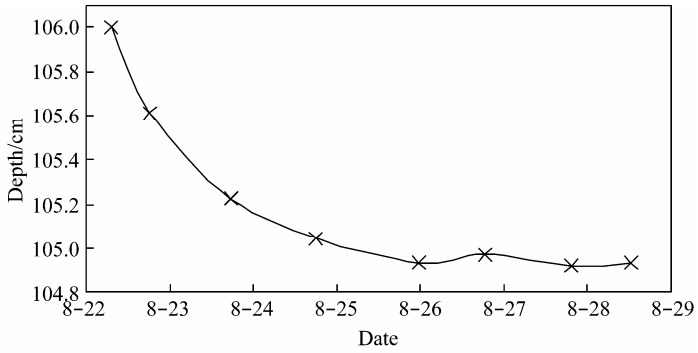

Figure 6 Variations in the base of the floe.

3 Discussions and Conclusions

During the camp period of the third CHINARE-Arctic cruise, the surface air temperature remained below 0℃, most leads around the investigated floe were frozen up and the sea-ice bottom reached its mass balance. All of these phenomena implied that sea ice in this region had commenced its annual cycle of growth during the camp period. The broadband albedo over 320— 950 nm of the thin ice over a small lead was 0.46 ±0.03, which was smaller than that of normal bare or snow covered ice, but larger than that of open water evidently. The seawater temperature in the lead was relatively warm prior to freezing, after which it cooled down gradually, and ultimately decreased to about −1.4℃. The sea-ice lateral remained in its melting stage, with a melting rate responding to a equivalent latent heat flux of 21 ±6 W/m^2. As both the vertical and horizontal conductive heat fluxes were close to zero, the mass balance of the ice bottom was primarily controlled by the upwelling oceanic heat flux, while that of the ice lateral was primarily controlled by the lateral and upwelling oceanic heat fluxes and the irradiation transmitted through the lead. This discrepancy in the energy source can explain why there was a large difference between the ice bottom mass balance and its lateral mass balance during the same season.

The measurement system introduced in this study is still in the developmental stage, and many of the techniques employed must be further improved to enable the collection of sufficient data to parameterize the thermodynamic process of a floe-lead system. Specifically, for the system described here it is still necessary (1) to improve the precision and stability, and to realize automatic

measurements of the ice bottom and lateral mass balance; (2) to enhance the measurements of the radiation and turbulent heat fluxes over the lead; (3) to enhance the measurements of the irradiance transmittances through the lead and the ice cover to evaluate the role of irradiance transmittance on the ice mass balance; (4) and to enhance the measurements of seawater salinity in the lead and under the ice to characterize the disturbance of ice growth and decay on the salinity field of the upper ocean.

Acknowledgments The third CHINARE-Arctic cruise in 2008 was a part of the IPY 2007-2008 Program of China. This work was financially supported by the National Natural Science Foundation of China (Grant no. 40930848), the Norwegian Research Council (AMORA, 193592/S30), the China Postdoctoral Science Foundation (Grant no. 20100470400), and the International Cooperation Project of the Chinese Arctic and Antarctic Administration, SOA (Grant no. IC2010007). The RAMSES ACC-2 VIS hyper-spectral radiometer was provided by the Norwegian Polar Institute.

References

1 Comiso J C, Parkinson C L, Gersten R, et al. Accelerated decline in the Arctic sea ice cover. Geophys Res Lett, 2008, 35, L01703, doi:10.1029/2007GL031972
2 Haas C, Pfaffling A, Hendricks S, et al. Reduced ice thickness in Arctic Transpolar Drift favors rapid ice retreat. Geophys Res Lett, 2008, 35, L17501, doi:10.1029/2008GL034457
3 Lu P, Li Z, Cheng B, et al. Sea ice surface features in Arctic summer 2008: Aerial observations. Remote Sens Environ, 2010, 114: 693–699
4 Perovich D K, Light B, Eicken H, et al. Increasing solar heating of the Arctic Ocean and adjacent seas, 1979–2005: Attribution and role in the ice-albedo feedback. Geophys Res Lett, 2007, 34, L19505, doi:10.1029/2007GL031480
5 Sorteberg A, Katsov V, Walsh J E, et al. The Arctic Surface Energy Budget as Simulated with the IPCC AR4 AOGCMs. Clim Dynam, 2007, 29: 131–156
6 Parkinson C L, Washington W M. A large-scale numerical model of sea ice. J Geophys Res, 1979, 84(C1): 311–337
7 Perovich D K, Richter-Menge J A. From points to poles: extrapolating point measurements of sea-ice mass balance. Ann Glaciol, 2006, 44: 188–192
8 Lei R, Li Z, Cheng Y, et al. A new apparatus for monitoring sea ice thickness based on the Magnetostrictive-Delay-Line principle. J Atmos Oceanic Technol, 2009, 26(4): 818–827
9 Bian L, Gao Z, Lu L, et al. Observational estimation of heat budgets on drifting ice and open water over the Arctic Ocean. Sci China, Ser D, 2003, 46(6): 580–591
10 Perovich D K, Elder B C. Estimates of ocean heat flux at SHEBA. Geophys Res Lett, 2002, 29(9), 1344, doi:10.1029/2001GL014171
11 Li Z, Zhang Z, Dong X, et al. New techniques for monitoring the key parameters of the sea-ice mass balance in Arctic. Prog Nat Sci, 2004, 14(9): 1077–1080(In Chinese)
12 Lei R B, Li Z J, Zhang Z H, et al. Summer fast ice evolution off Zhongshan Station, Antarctica. Chin J Polar Sci, 2008, 19 (1): 54–62
13 Nicolaus M, Hudson S R, Gerland S, et al. A modern concept for autonomous and continuous measurements of spectral albedo and transmittance of sea ice. Cold Regs Sci Technol, 2010, 62: 14–28
14 Perovich D K, Grenfell T C, Light B, et al. Seasonal evolution of the albedo of multiyear Arctic sea ice. J Geophys Res, 2002, 107(C10), 8044, doi: 10.1029/2000JC000438
15 Lei R, Li Z, Cheng B, et al. Annual cycle of landfast sea ice in Prydz Bay, east Antarctica. J Geophys Res, 2010, doi:10.1029/2008JC005223
16 Yen Y C. Review of thermal properties of snow, ice and sea ice. Cold Regions Research and Engineering Laboratory Report 81−10, Hanover, New Hampshire, 1981: 1– 27